Critical times in multilayer diffusion. Part 1: Exact solutions

R. I. Hickson[a], S. I. Barry[*,a,b], G. N. Mercer[a,b]

[a] *School of Physical, Environmental and Mathematical Sciences, University of New South Wales at ADFA, Northcott Drive, Canberra, ACT 2600, AUSTRALIA*
[b] *National Centre for Epidemiology and Public Health, Australian National University, Canberra, ACT 0200, AUSTRALIA*

Abstract

While diffusion has been well studied, diffusion across multiple layers, each with different properties, has had less attention. This type of diffusion may arise in heat transport across composite materials or layered biological material. Usually of most interest is a critical time, such as the time for a material to heat up. Here an exact solution is found which demonstrates the critical time behaviour for transport across multiple layers. This solution illustrates the limitations of traditional averaging methods.

Key words: Diffusion, Multilayer, Critical time, Time lag, Laminates, Composite materials

[*]Corresponding author. Tel.: +61 2 6125 9506; fax: +61 6125 0740
Email addresses: R.I.Hickson@gmail.com (R. I. Hickson), Steven.Barry@anu.edu.au (S. I. Barry)

Nomenclature			
α	proportion of the steady state	n	total number of layers
$D = d^2$	single layer diffusivity	t	time
$D_{\text{av}} = d_{\text{av}}^2$	average diffusivity	t_{av}	typical critical time
$D_i = d_i^2$	layer diffusivity	t_c	multilayer critical time
$f(x)$	initial condition	t_s	single layer critical time
i	layer index	θ_1	boundary condition at $x = x_0$
L	total length of medium	θ_2	boundary condition at $x = x_n$
l_i	layer width	$U(x,t)$	temperature
λ_m	multilayer eigenvalues	$v(x,t)$	transient solution
m	eigenvalue index	$w(x)$	steady state solution
μ_m	single layer eigenvalues	x	spatial position
H_i	contact transfer coefficient		
$[A, B]$	shorthand for $n/2$ biperiodic layers, material properties D_A, D_B as $ABAB\ldots AB$		

1. Introduction

Diffusion through multiple layers has applications to a wide range of areas in heat and mass transport. Industrial applications include annealing steel coils (7; 24; 33), the performance of semiconductors (2) and electrodes (9; 11), and geological profiles (16). Biological applications include determining the effectiveness of drug carriers inserted into living tissue (31), the probing of biological tissue with infrared light (22), and analysing the heat production of muscle (14).

For multilayer diffusion across n layers the standard diffusion equation,

$$\frac{\partial U_i}{\partial t} = D_i \frac{\partial^2 U_i}{\partial x^2}\,, \quad i \in [1, n]\,, \tag{1}$$

is applicable in each layer where $x_{i-1} \leq x \leq x_i$ is distance, U_i is the temperature in layer i at time t, and D_i is the diffusivity of layer i, as shown in Figure 1. For clarity, in subsequent sections the notation $d_i \equiv \sqrt{D_i}$ is also used.

Exact solutions for diffusion in layered media have been found for diverse applications and geometries. These include solutions in Cartesian coordinates for two layers (29; 30; 31) and n layers (12; 17; 27; 28; 32), and cylindrical n layer solutions (13; 21). Many of these publications use separation methods similar to that outlined in Sections 2 and 3 of this article. However previous publications that use separation methods, and also consider Cartesian coordinates, assume perfect contact between the layers (12; 17; 27; 28; 32) and some (12; 17; 32) have less general boundary conditions. Laplace transform approaches are also used (5; 9), but are less common due to the difficulty of the inverse transform, which are often only numerically found.

An important aspect of multilayer diffusion is the 'critical time', which is a measure of how long the diffusive process takes. This is important for a number of applications, such as the 'time to heat' when annealing steel coils (7; 24; 33). There are multiple definitions of critical time since mathematically, an infinite amount of time is required to reach steady state (20). A common definition is the time when the average temperature reaches a proportion of the average steady state. That is, the value of $t = t_c$ such that

$$\int_{x=0}^{L} U(x, t_c)\, dx = \alpha \int_{x=0}^{L} w(x)\, dx\,, \tag{2}$$

where $U(x,t)$ is the temperature, $0 < \alpha < 1$ is a chosen constant, and $w(x)$ is the steady state. Landman and McGuinness (20) summarise previous work and applications using this critical time definition, also called the mean action time (25; 26).

The most common approximation of critical time (see for example (3; 6; 15; 19)), is the simple expression

$$t_{\text{av}} = \frac{L^2}{6D_{\text{av}}}\,, \tag{3}$$

where D_{av} is the commonly averaged diffusivity for layered materials, given by

$$\frac{L}{D_{\text{av}}} = \sum_{i=1}^{n} \frac{l_i}{D_i}\,. \tag{4}$$

Here L is the total medium length, and l_i are the lengths of each layer with material diffusivity D_i. This series-averaged diffusivity is a valid measure when calculating heat fluxes at steady state, or for a large number of layers. The critical time, Equation (3), corresponds to the critical time definition given in Equation (2) for $\alpha \approx 0.8435$, a result calculated in Section 2. However, Equation (3) is only valid for a single layered material. Absi *et al.* (1) describe a brief numerical and experimental comparison using Equation (3) versus the full coupled numerical system for two layers. Their results indicate the limitations of this formula, a result we corroborate in our numerical simulation shown in Figure 3.

Several publications have attempted to calculate a diffusive critical time through composites, in Cartesian, cylindrical and spherical geometries with

Ash *et al.* (3; 4) giving detailed solutions. These are summarised in Barrer (6) for some of the usual layer configurations, such as two repeated layers, $ABAB\ldots$, also referred to as a 'biperiodic region'. Their complicated derivation is equivalent to choosing $\alpha \approx 0.8435$ in Equation (2). However, as shown in our companion paper Hickson *et al.* (18), their result for a one-dimensional Cartesian layered material does not reflect the actual critical time. Aguirre *et al.* (2) determined a solution for sinusoidally imposed temperature, calculating an effective diffusivity for a composite material. Their result is an improved version of the series-averaged diffusivity given in Equation (4). The effective diffusivity was found in terms of the imposed frequency where Equation (4) is reflected in the low frequency limit when the material is in quasi-steady state.

We will show the standard Equations (3) and (4) give inaccurate results. The exact solution is found for diffusion in a one-dimensional Cartesian material with only one layer in Section 2. This is extended to the more complicated multilayer case in Section 3 where the solutions are also verified. The critical time is calculated numerically in Section 4 and discussed in Section 5.

2. Single layer solution

In this section we find an exact solution for the single layer case. Whilst not original, this will demonstrate the solution method used for the more difficult multilayer diffusion problem in Section 3. Additionally, these results will assist in understanding the definition and behaviour of critical time.

The single layer case is depicted in Figure 2, where

$$\frac{\partial U}{\partial t} = D\frac{\partial^2 U}{\partial x^2}\,, \tag{5}$$

for some initial condition, $U(x,0) = f(x)$, and mixed boundary conditions,

$$\begin{aligned} a_1 U + b_1 \frac{\partial U}{\partial x} &= \theta_1 \qquad \text{at} \quad x = x_0\,, \\ a_2 U + b_2 \frac{\partial U}{\partial x} &= \theta_2 \qquad \text{at} \quad x = x_1\,, \end{aligned} \tag{6}$$

where a_1, a_2, b_1, b_2, θ_1 and θ_2 are constants.

Due to the boundary conditions the problem must be split into the steady state, $w(x)$, and transient, $v(x,t)$, components (8) where $U(x,t) = w(x) + v(x,t)$. The steady state solution is found by integrating and substituting in the boundary conditions to give

$$w(x) = \frac{(a_1\,\theta_2 - a_2\,\theta_1)(x - x_0) + \theta_1(a_2\,L + b_2) - b_1\,\theta_2}{a_1\,a_2\,L + a_1\,b_2 - a_2\,b_1}\,. \tag{7}$$

It has been assumed that a_1 and a_2 cannot both be zero. If $a_1 = 0 = a_2$ then a solution only exists if $b_2\,\theta_1 = b_1\,\theta_2$; otherwise the finite medium has an unbalanced heat input giving rise to unbounded temperature.

The transient solution, $v(x,t)$, satisfies

$$\frac{\partial v}{\partial t} = D\frac{\partial^2 v}{\partial x^2}\,, \tag{8}$$

$$a_1 v + b_1 \frac{\partial v}{\partial x} = 0 \qquad \text{at} \quad x = x_0\,, \tag{9}$$

$$a_2 v + b_2 \frac{\partial v}{\partial x} = 0 \qquad \text{at} \quad x = x_1\,, \tag{10}$$

$$v(x,0) = g(x)\,, \tag{11}$$

where $g(x) = f(x) - w(x)$. This can be solved using separation of variables where $v(x,t) = X(x)T(t)$, resulting in the two eigenfunction solutions

$$X(x) = \sin\left(\frac{\mu_m}{d}(x - x_0)\right) - \frac{b_1\mu_m}{a_1\,d}\cos\left(\frac{\mu_m}{d}(x - x_0)\right)\,, \tag{12}$$

$$T(t) = e^{-\mu_m^2 t}\,, \tag{13}$$

where we use the simpler notation $d = \sqrt{D}$ and the eigenvalues, μ_m, satisfy

$$\sin\left(\frac{\mu_m L}{d}\right)\left[\frac{a_1\, a_2\, d}{\mu_m} + \frac{b_1\, b_2\, \mu_m}{d}\right] + \cos\left(\frac{\mu_m L}{d}\right)[a_1\, b_2 - a_2\, b_1] = 0\,. \quad (14)$$

Therefore the transient solution is

$$v(x,t) = \sum_{m=1}^{\infty} A_m e^{-\mu_m^2 t} X(x)\,, \quad (15)$$

where A_m is determined by Sturm–Liouville theory as

$$A_m = \frac{\displaystyle\int_{x_0}^{x_1} g(x) X(x)\, dx}{\displaystyle\int_{x_0}^{x_1} X^2(x)\, dx}\,. \quad (16)$$

Hence the complete solution is

$$U(x,t) = w(x) + \sum_{m=1}^{\infty} A_m e^{-\mu_m^2 t} X(x)\,. \quad (17)$$

Equation (2) can now be written as

$$(1-\alpha)\int_{x=x_0}^{x_1} w(x)\, dx + \int_{x=x_0}^{x_1} v(x,t_s)\, dx = 0\,, \quad (18)$$

for the critical time, $t = t_s$.

For illustrative purposes we consider the simpler case of constant boundary conditions, where $a_1 = 1 = a_2$ and $b_1 = 0 = b_2$ in Equation (6). These give $\mu_m = m\pi d/L$ and when $f(x) = 0$, $A_m = 2(\theta_2(-1)^m - \theta_1)/(m\pi)$. The critical time is then evaluated using Equation (17) to give

$$(1-\alpha)(\theta_1+\theta_2) + 4\sum_{m=1}^{\infty} \frac{[1+(-1)^{m+1}]}{(m\pi)^2}\,[\theta_2(-1)^m - \theta_1]\, e^{-\mu_m^2 t_s} = 0\,. \quad (19)$$

Due to the infinite sum over the eigenvalues, Equation (19) cannot explicitly be solved for the critical time, t_s. However for large enough times this solution is dominated by the leading order eigenvalue. Hence if only the leading

eigenvalue is considered, when $m = 1$, Equation (19) can be rearranged to give

$$t_s \approx \frac{L^2}{\pi^2 D} \log \left\{ \frac{8}{\pi^2 (1-\alpha)} \right\} . \tag{20}$$

The critical time must be positive, therefore $(1 - 8/\pi^2) < \alpha < 1$. Equating this to Equation (3) gives $\alpha = 1 - (8/\pi^2)\exp(-\pi^2/6) \approx 0.8435$.

Similarly, for an insulated boundary at $x = x_1$, where $a_1 = 1$, $a_2 = 0$, $b_1 = 0$, $b_2 = 1$ and $\theta_2 = 0$ in Equation (6), the critical time for the leading eigenvalue is

$$t_s \approx \frac{4L^2}{\pi^2 D} \log \left\{ \frac{8}{\pi^2 (1-\alpha)} \right\} . \tag{21}$$

Equating this to Equation (3) gives $\alpha = 1 - (8/\pi^2)\exp(-\pi^2/24) \approx 0.4627$. The difference between Equations (20) and (21) is of interest, as it shows that insulation allows the medium to reach the critical temperature four times more quickly.

3. Multilayer solutions

In this section the multilayer solution for general boundary conditions are found using the same method as the single layer, by splitting the solution into the steady state, $w_i(x)$, and transient, $v_i(x,t)$, components.

The contact between layers is often imperfect giving rise to a jump condition between layers represented by

$$D_i \frac{\partial U_i}{\partial x} = H_i \left(U_{i+1} - U_i \right) , \tag{22}$$

$$D_{i+1} \frac{\partial U_{i+1}}{\partial x} = H_i \left(U_{i+1} - U_i \right) , \tag{23}$$

at $x = x_i$ for $i = 1, 2, \ldots, (n-1)$ where H_i is the contact transfer coefficient. This reflects roughness (7) and contact resistance (8). If $H_i \to \infty$ then con-

tact becomes perfect and hence this limit represents the equivalent matching conditions

$$U_i(x_i,t) = U_{i+1}(x_i,t)\,, \tag{24}$$

$$D_i \left.\frac{\partial U_i}{\partial x}\right|_{x_i} = D_{i+1} \left.\frac{\partial U_{i+1}}{\partial x}\right|_{x_i}\,, \tag{25}$$

which represent continuity in 'temperature' and flux respectively.

After Equation (1) has been split into steady state and transient parts, the steady state solution, $w_i(x)$, satisfies

$$D_i \frac{\partial^2 w_i}{\partial x^2} = 0\,, \tag{26}$$

$$a_1 w_1 + b_1 \frac{\partial w_1}{\partial x} = \theta_1 \qquad \text{at} \quad x = x_0\,, \tag{27}$$

$$a_2 w_n + b_2 \frac{\partial w_n}{\partial x} = \theta_2 \qquad \text{at} \quad x = x_n\,, \tag{28}$$

$$D_i \frac{\partial w_i}{\partial x} = H_i\,(w_{i+1} - w_i)\,, \tag{29}$$

$$D_{i+1} \frac{\partial w_{i+1}}{\partial x} = H_i\,(w_{i+1} - w_i)\,. \tag{30}$$

Integrating Equation (26) results in

$$w_i(x) = q_i(x - x_{i-1}) + h_i\,, \tag{31}$$

where q_i and h_i are constants. Using the boundary conditions, Equations (27) and (28), respectively give

$$h_1 = \frac{\theta_1 - b_1\,q_1}{a_1}\,,$$

$$(a_2\,l_n + b_2)\,q_n + a_2\,h_n = \theta_2\,, \tag{32}$$

and the interface conditions, Equations (29) and (30), result in recursively

defined constants:

$$q_{i+1} = \frac{D_i}{D_{i+1}} q_i = \frac{D_1}{D_{i+1}} q_1 \,, \tag{33}$$

$$h_{i+1} = h_i + q_i \left(\frac{D_i}{H_i} + l_i \right) = h_1 + \sum_{j=1}^{i} \left(\frac{D_j}{H_j} + l_j \right) q_j \,. \tag{34}$$

These are used to calculate q_n and h_n, which are substituted back into Equation (32) to find q_1. After some algebra,

$$q_1 = \frac{(a_1\theta_2 - a_2\theta_1) D_n}{a_1 b_2 D_1 - a_2 b_1 D_n + a_1 a_2 D_1 D_n \left(\dfrac{L}{D_{\text{av}}} + \displaystyle\sum_{j=1}^{n-1} \dfrac{1}{H_j} \right)} \,, \tag{35}$$

$$q_i = \frac{D_1}{D_i} \, q_1 \,, \tag{36}$$

$$h_i = h_1 + D_1 q_1 \sum_{j=1}^{i-1} \left(\frac{l_j}{D_j} + \frac{1}{H_j} \right) \,. \tag{37}$$

The inclusion of D_{av} in Equation (35) is interesting as it shows averaging of the material properties.

The transient solution, $v_i(x,t)$, satisfies

$$\frac{\partial v_i}{\partial t} = D_i \frac{\partial^2 v_i}{\partial x^2} \,, \tag{38}$$

$$a_1 v_1 + b_1 \frac{\partial v_1}{\partial x} = 0 \qquad \text{at} \quad x = x_0 \,, \tag{39}$$

$$a_2 v_n + b_2 \frac{\partial v_n}{\partial x} = 0 \qquad \text{at} \quad x = x_n \,, \tag{40}$$

$$D_i \frac{\partial v_i}{\partial x} = H_i \left(v_{i+1} - v_i \right) \,, \tag{41}$$

$$D_{i+1} \frac{\partial v_{i+1}}{\partial x} = H_i \left(v_{i+1} - v_i \right) \,. \tag{42}$$

$$v_i(x,0) = f_i(x) - w_i(x) = g_i(x) \,. \tag{43}$$

Using separation of variables, where $v_i(x,t) = X_i(x)T(t)$, results in the two

eigenfunction solutions

$$X_i(x) = K_{1,i}\sin\left(\frac{\lambda_m}{d_i}(x-x_{i-1})\right) + K_{2,i}\cos\left(\frac{\lambda_m}{d_i}(x-x_{i-1})\right), \quad (44)$$

$$T(t) = e^{-\lambda_m^2 t}, \quad (45)$$

where $K_{1,i}$ and $K_{2,i}$ are constants, λ_m are the eigenvalues, and $X_i(x) \equiv X_{i,m}(x)$. Applying the boundary and interface conditions to Equation (44) results in a series of expressions that can be rewritten in terms of one of the constants, chosen here as $K_{1,1}$. Hence in Equation (44), $K_{1,1} = 1$ by definition of the chosen constant, from Equation (39)

$$K_{2,1} = \frac{-b_1\lambda_m}{a_1 d_1}, \quad (46)$$

from Equation (42)

$$K_{1,i+1} = \frac{d_i}{d_{i+1}}\left[K_{1,i}\cos\left(\lambda_m\frac{l_i}{d_i}\right) - K_{2,i}\sin\left(\lambda_m\frac{l_i}{d_i}\right)\right], \quad (47)$$

from Equation (41)

$$\begin{aligned} K_{2,i+1} &= K_{1,i}\left[\sin\left(\lambda_m\frac{l_i}{d_i}\right) + \frac{\lambda_m d_i}{H_i}\cos\left(\lambda_m\frac{l_i}{d_i}\right)\right] \\ &\quad + K_{2,i}\left[\frac{-\lambda_m d_i}{H_i}\sin\left(\lambda_m\frac{l_i}{d_i}\right) + \cos\left(\lambda_m\frac{l_i}{d_i}\right)\right], \end{aligned} \quad (48)$$

and the eigenvalues, λ_m, are defined by the transcendental expression

$$\begin{aligned} &K_{1,n}\left[a_2\sin\left(\lambda_m\frac{l_n}{d_n}\right) + \frac{\lambda_m b_2}{d_n}\cos\left(\lambda_m\frac{l_n}{d_n}\right)\right] \\ &+K_{2,n}\left[-\frac{\lambda_m b_2}{d_n}\sin\left(\lambda_m\frac{l_n}{d_n}\right) + a_2\cos\left(\lambda_m\frac{l_n}{d_n}\right)\right] = 0, \end{aligned} \quad (49)$$

which comes from Equation (40). Note $K_{1,i}$ and $K_{2,i}$ are recursively defined. The transient solution is then

$$v_i(x,t) = \sum_{m=1}^{\infty} C_m e^{-\lambda_m^2 t} X_i(x). \quad (50)$$

Using the initial condition,

$$v_i(x,0) = g_i(x) = \sum_{m=1}^{\infty} C_m X_i(x)\,, \tag{51}$$

so to solve for the summation constant, C_m, a suitable orthogonality condition must be used. The following orthogonality condition is proven in Appendix A,

$$\sum_{i=1}^{n} \int_{x_{i-1}}^{x_i} X_i(x,m)\, X_i(x,p)\, dx \;\; = \;\; \begin{cases} 0, & m \neq p \\ \kappa, & m = p \end{cases} \tag{52}$$

where κ is a constant. Using this gives

$$C_m = \frac{\displaystyle\sum_{i=1}^{n} \int_{x_{i-1}}^{x_i} g_i(x) X_i(x)\, dx}{\displaystyle\sum_{i=1}^{n} \int_{x_{i-1}}^{x_i} X_i^2(x)\, dx}\,. \tag{53}$$

The complete solution is therefore

$$U_i(x,t) = w_i(x) + \sum_{m=1}^{\infty} C_m e^{-\lambda_m^2 t} X_i(x)\,. \tag{54}$$

We will now investigate the case of $H_i \to \infty$; when the jump interface solution approaches the matching interface solution. First consider the steady state coefficients, Equations (35) and (37). As $H_i \to \infty$,

$$q_1 = \frac{(a_1\theta_2 - a_2\theta_1)D_n}{a_1 b_2 D_1 - a_2 b_1 D_n + a_1 a_2 D_1 D_n \left(\dfrac{L}{D_{\text{av}}}\right)} \tag{55}$$

and

$$h_i = h_1 + D_1 q_1 \sum_{j=1}^{i-1} \frac{l_j}{D_j}\,. \tag{56}$$

The only equation involving the jump for the transient solution is Equation (48). As $H_i \to \infty$,

$$K_{2,i+1} = K_{1,i} \sin\left(\lambda_m \frac{l_i}{d_i}\right) + K_{2,i} \cos\left(\lambda_m \frac{l_i}{d_i}\right) . \tag{57}$$

The critical time for multiple layers, t_c, is found by solving the equivalent multilayer version of Equation (18):

$$(1-\alpha) \sum_{i=1}^{n} \int_{x_{i-1}}^{x_i} w_i(x)\, dx + \sum_{i=1}^{n} \int_{x_{i-1}}^{x_i} v_i(x, t_c)\, dx = 0 . \tag{58}$$

Substituting the multilayer solution, Equation (54), into this gives

$$(1-\alpha) \sum_{i=1}^{n} \left\{ h_i\, l_i + \frac{q_i\, l_i^2}{2} \right\} + \sum_{i=1}^{n} d_i \sum_{m=1}^{\infty} \frac{C_m}{\lambda_m} e^{-\lambda_m^2 t_c} \Psi_{i,m} = 0 , \tag{59}$$

where

$$\Psi_{i,m} = K_{1,i} \left\{ 1 - \cos\left(\frac{\lambda_m l_i}{d_i}\right) \right\} + K_{2,i} \sin\left(\frac{\lambda_m l_i}{d_i}\right) . \tag{60}$$

Although this could be approximated using the leading eigenvalue, as done in Section 2, the expression is still complicated and does not provide further insight to the multilayer critical time behaviour. However, the critical time can be calculated numerically using Equation (59), and is denoted the 'exact' critical time in later analysis.

The solutions given by Equations (17) and (54) were verified for multiple scenarios using two different numerical schemes. The first scheme used finite differences, explained in Appendix B, and was implemented in MATLAB (23). The second uses the commercial finite elements package FlexPDE (10). Agreement between the two numerical schemes and the analytical solutions were found to within expected numerical accuracy.

4. Numerical results

To explore the behaviour of the multilayer critical time a biperiodic region is considered, with $n/2$ repeating layers with 'A' and 'B' properties such as layer width, l_A and l_B, and diffusivity, D_A and D_B. That is, there are n layers in total with repeated layers $ABAB \dots AB$, denoted by shorthand as $[A, B]$ or equivalently $[D_A, D_B]$. The region is defined with $x_0 = 0$ to $x_n = 1$, hence $L = 1$. For simplicity here, equal widths for both layers are used, so $l_i = 1/n$, but in general this is not necessary. Different diffusivities are used in each layer, where the larger diffusivity $D = 1$ and the smaller diffusivity $D = 0.1$. The initial condition used is $f_i(x) = 0$ and the proportion of the steady state is $\alpha = 0.5$.

Constant boundary conditions are used for Figure 3, where $a_1 = 1 = a_2$ and $b_1 = 0 = b_2$, $\theta_1 = 1$ and $\theta_2 = 0$, and continuous interface conditions are used, where $H_i \to \infty$. Three different scenarios are presented in Figure 3 for the critical time as a function of the number of repeated layers, $n/2$. The first scenario uses [1, 0.1] periodic layers, and the second scenario uses [0.1, 1]. The third 'Single Dav' scenario averages the diffusivities using Equation (4), and calculates the critical time for the single layer solution, Equation (20). Of interest is the convergence of the 'Exact [1, 0.1]' and 'Exact [0.1, 1]' scenarios from different sides of the averaged solution and the local maxima for the 'Exact [0.1, 1]' scenario.

Similar scenarios are explored in Figure 4, but for different boundary conditions. The boundary at $x = x_0$ is made constant, with $a_1 = 1$, $b_1 = 0$ and $\theta_1 = 1$, and the boundary at $x = x_n$ is insulated, with $a_2 = 0$, $b_2 = 1$ and $\theta_2 = 0$. The value the critical times are converging to are noticeably different

for Figures 3 and 4. Also, both the 'Exact [1, 0.1]' and 'Exact [0.1, 1]' scenarios are symmetric about the 'Single Dav' scenario for Figure 4. Note the 'Exact [0.1, 1]' solution does not give a local maximum as in Figure 3.

Both Figure 3 and 4 demonstrate that a relatively large number of layers are required for accurate results when using the traditional averaging approach, Equation (3). In particular, the averaging method is very poor for less then ten repeated layers, or twenty layers in total.

Although the numerical implementations provide some insight as to how the behaviour differs for multiple layers as opposed to a single layer, it fails to explain why this difference occurs. Hence in Hickson *et al.* (18) we explore an approximate perturbation of the exact solution which will illuminate this behaviour, and explain the local maximum found in the 'Exact [0.1, 1]' scenario in Figure 3.

5. Discussion

The most interesting point illustrated with this work is that layered materials do not exhibit symmetric properties. That is, the time taken to diffuse depends greatly on which order the materials are layered. Hence this work can be used to consider the inverse problem, where it is possible to apply the critical time to determine the individual properties of the layered materials. That is, two measurements of critical time, with the material direction switched, are sufficient to determine the properties of each individual layer.

Although only one definition for critical time has been explored here, it is possible to apply the exact solutions found to alternative definitions. The method used to find the exact solutions is extendable to cylindrical and

spherical coordinates.

6. Conclusion

Exact solutions were found for multilayer diffusion, with general boundary and interface conditions. These solutions were then used to numerically demonstrate the limitations of the traditional averaging methods, Equations (3) and (4). We demonstrated the nearly symmetric behaviour of critical time with number of layers and the importance of the layer order.

A. Proof of orthogonality condition

The orthogonality condition for n-layers is proven here using standard Sturm-Liouville theory. The original eigenfunction equation, which results from the separation of Equation (38), is

$$\frac{\partial^2 X_{i,m}}{\partial x^2} = \frac{\varphi_m}{D_i} X_{i,m}\,, \quad i \in [1, n]\,, \tag{61}$$

for the ith layer and mth eigenvalue, where $\varphi_m = -\lambda_m^2$. Multiplying both sides of Equation (61) by $X_{i,p}$, for the pth eigenvalue where $m \neq p$, and integrating gives

$$\int_{x_{i-1}}^{x_i} X_{i,p}\, X''_{i,m}\, dx = \frac{\varphi_m}{D_i} \int_{x_{i-1}}^{x_i} X_{i,p}\, X_{i,m}\, dx \tag{62}$$

and similarly, for the other eigenvalue,

$$\int_{x_{i-1}}^{x_i} X_{i,m}\, X''_{i,p}\, dx = \frac{\varphi_p}{D_i} \int_{x_{i-1}}^{x_i} X_{i,m}\, X_{i,p}\, dx\,. \tag{63}$$

Subtracting Equation (63) from Equation (62), using integration by parts and simplifying gives

$$\begin{aligned}(\varphi_m - \varphi_p) \int_{x_{i-1}}^{x_i} X_{i,m}\, X_{i,p}\, dx &= D_i \left(\left[X_{i,p}\, X'_{i,m} \right]_{x_{i-1}}^{x_i} - \left[X_{i,m}\, X'_{i,p} \right]_{x_{i-1}}^{x_i} \right) \\ &= D_i \left(X_{i,p}(x_i)\, X'_{i,m}(x_i) - X_{i,p}(x_{i-1})\, X'_{i,m}(x_{i-1}) \right. \\ &\quad \left. - X_{i,m}(x_i)\, X'_{i,p}(x_i) + X_{i,m}(x_{i-1})\, X'_{i,p}(x_{i-1}) \right) . \end{aligned} \tag{64}$$

The same is done for the '$i+1$'th layer,

$$\begin{aligned}(\varphi_m - \varphi_p) \int_{x_i}^{x_{i+1}} X_{i+1,m}\, X_{i+1,p}\, dx = \\ D_{i+1} \left(X_{i+1,p}(x_{i+1})\, X'_{i+1,m}(x_{i+1}) - X_{i+1,p}(x_i)\, X'_{i+1,m}(x_i) \right. \\ \left. - X_{i+1,m}(x_{i+1})\, X'_{i+1,p}(x_{i+1}) + X_{i+1,m}(x_i)\, X'_{i+1,p}(x_i) \right) . \end{aligned} \tag{65}$$

The internal boundary conditions are

$$X_{i,m}(x_i) = X_{i+1,m}(x_i) , \tag{66}$$

$$D_i \left. \frac{\partial X_{i,m}}{\partial x} \right|_{x_i} = D_{i+1} \left. \frac{\partial X_{i+1,m}}{\partial x} \right|_{x_i} , \tag{67}$$

for $i \in [1, n-1]$. Using these, Equation (65) becomes

$$\begin{aligned}(\varphi_m - \varphi_p) \int_{x_i}^{x_{i+1}} X_{i+1,m}\, X_{i+1,p}\, dx = \\ D_{i+1} X_{i+1,p}(x_{i+1})\, X'_{i+1,m}(x_{i+1}) - D_i X_{i,p}(x_i)\, X'_{i,m}(x_i) \\ - D_{i+1} X_{i+1,m}(x_{i+1})\, X'_{i+1,p}(x_{i+1}) + D_i X_{i,m}(x_i)\, X'_{i,p}(x_i) . \end{aligned} \tag{68}$$

Adding Equations (64) and (68) then gives

$$\begin{aligned}(\varphi_m - \varphi_p) \left[\int_{x_{i-1}}^{x_i} X_{i,m}\, X_{i,p}\, dx + \int_{x_i}^{x_{i+1}} X_{i+1,m}\, X_{i+1,p}\, dx \right] = \\ X_{i,m}(x_{i-1})\, X'_{i,p}(x_{i-1}) - X_{i,p}(x_{i-1})\, X'_{i,m}(x_{i-1}) \\ + X_{i+1,p}(x_{i+1})\, X'_{i+1,m}(x_{i+1}) - X_{i,m}(x_{i+1})\, X'_{i,p}(x_{i+1}) . \end{aligned}$$

Therefore the middle, x_i, points are always going to cancel out, leaving only the end points, $x = x_0$ and $x = x_n$. That is,

$$\begin{aligned}(\varphi_m - \varphi_p) \sum_{i=1}^{n} \int_{x_{i-1}}^{x_i} X_{i,m}\, X_{i,p}\, dx = \\ X_{1,m}(x_0)\, X'_{1,p}(x_0) - X_{1,p}(x_0)\, X'_{1,m}(x_0) \\ + X_{n,p}(x_n)\, X'_{n,m}(x_n) - X_{n,m}(x_n)\, X'_{n,p}(x_n)\,. \end{aligned} \tag{69}$$

Given general boundary conditions at $x = x_0$:

$$\begin{aligned} a_1 X_{1,m}(x_0) + b_1 X'_{1,m}(x_0) &= 0 \\ a_1 X_{1,p}(x_0) + b_1 X'_{1,p}(x_0) &= 0 \end{aligned} \tag{70}$$

then for a_1 and b_1 both non-zero this requires the determinant

$$X_{1,m}(x_0) X'_{1,p}(x_0) - X_{1,p}(x_0) X'_{1,m} = 0 \tag{71}$$

and similarly at $x = x_n$. Hence Equation (69) becomes

$$(\varphi_m - \varphi_p) \sum_{i=1}^{n} \int_{x_{i-1}}^{x_i} X_{i,m}\, X_{i,p}\, dx = 0\,.$$

When $\varphi_m \neq \varphi_p$,

$$\sum_{i=1}^{n} \int_{x_{i-1}}^{x_i} X_{i,m}\, X_{i,p}\, dx = 0$$

and hence the orthogonality condition has been proven.

This proof is extendable to the jump interface conditions, Equation (23), although with more complicated algebra.

B. Finite difference scheme for layers

The finite difference scheme uses second order central differences with an Euler time step. An added complexity arises from the layered nature of the

problem. Figure 5 depicts an interface between layers with nomenclature and indexing. The inner points of a layer use the standard first order time and second order space finite differencing, that is

$$\frac{\partial U_{j-1}}{\partial t} = \frac{D_i}{\Delta x^2} \left[U_{j-2} - 2U_{j-1} + U_j \right] , \tag{72}$$

where U_j is the temperature at the spatial point j in layer i. The point on the interface is found using the flux matching condition, Equation (25), as

$$\frac{\partial U_j}{\partial t} = \frac{1}{\Delta x^2} \left[D_i \, U_{j-1} - (D_i + D_{i+1}) \, U_j + D_{i+1} \, U_{j+1} \right] \tag{73}$$

where U_j lies on the intersection of the i and $(i+1)$ layers, as shown in Figure 5. Thus the differencing for this system can be illustrated by the following matrix

$$\frac{d}{dt} \begin{bmatrix} \vdots \\ U_{j-2} \\ U_{j-1} \\ U_j \\ U_{j+1} \\ U_{j+2} \\ \vdots \end{bmatrix} = \begin{bmatrix} & \ddots & & & & & \\ & & \ddots & & & & \\ \cdots & c_i & -2c_i & c_i & 0 & 0 & \cdots \\ \cdots & 0 & c_i & -c_i - c_{i+1} & c_{i+1} & 0 & \cdots \\ \cdots & 0 & 0 & c_{i+1} & -2c_{i+1} & c_{i+1} & \cdots \\ & & & & \ddots & & \\ & & & & & \ddots & \end{bmatrix} \begin{bmatrix} \vdots \\ U_{j-2} \\ U_{j-1} \\ U_j \\ U_{j+1} \\ U_{j+2} \\ \vdots \end{bmatrix} , \tag{74}$$

where $c_i = D_i/\Delta x$, and $c_{i+1} = D_{i+1}/\Delta x$. This is easily extended to multiple layers with numerous internal points and general boundary conditions. This can then be iterated in time using standard Euler time steps.

References

[1] J. Absi, D. S. Smith, B. Nait-Ali, S. Granjean, J. Berjonnaux, Thermal response of two-layer systems: Numerical simulation and experimental verification, *J. European Ceramic Soc.* **25**, 367–373, 2005.

[2] N. M. Aguirre, G. G. De La Cruz, Y. G. Gurevich, G. N. Logvinov, M. N. Kasyanchuk, Heat diffusion in two-layer structures: photoacoustic experiments, *Phys. Stat. Sol.* **220**, 781–787, 2000.

[3] R. Ash, R. M. Barrer, D. G. Palmer, Diffusion in multiple laminates, *Brit. J. Appl. Phys.* **16**, 873–884, 1965.

[4] R. Ash, R. M. Barrer, J. H. Petropoulos, Diffusion in heterogeneous media: properties of a laminated slab, *Brit. J. Appl. Phys.* **14**, 854–862, 1963.

[5] M. F. A. Azeez, A.F. Vakakis, Axisymmetric transient solutions of the heat diffusion problem in layered composite media, *Int. J. Heat. Mass Transf.* **43**, 3883–3895, 2000.

[6] R. M. Barrer, Diffusion and permeation in heterogenous media, *Diffusion in Polymers*, ed: J. Crank, G. S. Park, Academic Press, London, 165-215, 1968.

[7] S. I. Barry, W. L. Sweatman, Modelling heat transfer in steel coils, *ANZIAM J. (E)* **50**, C668–C68, 2009.

[8] H. S. Carslaw, J. C. Jaeger, *Conduction of heat in solids*, Clarendon Press, Oxford, 1959.

[9] J. Diard, N. Glandut, C. Montella, J. Sanchez, One layer, two layers, etc. An introduction to the EIS study of multilayer electrodes. Part 1: Theory, *J. Electroanalytical Chemistry* **578**, 247–257, 2005.

[10] FlexPDE, PDE Solutions Inc., Spokane Valley, `http://www.pdesolutions.com`.

[11] V. Freger, Diffusion impedance and equivalent circuit of a multilayer film, *Electrochemistry Communications* **7**, 957–961, 2005.

[12] M. Fukuda, H. Kawai, Diffusion of low molecular weight substances into a laminar film. 1: Rigorous solution of the diffusion equations in a composite film of multiple layers, *Polymer Engineering and Science* **35**, 8, 709–721, 1995.

[13] M. Fukuda, H. Kawai, Diffusion of low molecular weight substances into a fibre with skin-core structure – Rigorous solution of the diffusion equations in a coaxial cylinder of multiple components, *Polymer Engineering and Science* **34**, 4, 330–340, 1994.

[14] S. H. Gilbert, R. T. Mathias, Analysis of diffusion delay in a layered medium, *Biophys. J.* **54**, 603–610, 1988.

[15] G. L. Graff, R. E. Williford, P. E. Burrows, Mechanisms of vapor permeation through multilayer barrier films: Lag time versus equilibrium permeation, *J. Appl. Phys.* **96**(4), 1840–1849, 2004.

[16] P. Grossel, F. Depasse, Alternating heat diffusion in thermophysical depth profiles: multilayer and continuous descriptions, *J. Phys. D: Appl. Phys.* **31**, 216–223, 1998.

[17] R. I. Hickson, S. I. Barry, G. N. Mercer, Exact and numerical solutions for effective diffusivity and time lag through multiple layers, *ANZIAM J. (E)* **50**, C682–C695, 2009.

[18] R. I. Hickson, S. I. Barry, G. N. Mercer, Critical times in multilayer diffusion. Part 2: Approximate corrections, *Int. J. Heat Mass Transfer* (submitted), 2009.

[19] B. Kruczek, H. L. Frisch, R. Chapanian, Analytical solution for the effective time lag of a membrane in a permeate tube collector in which Knudsen flow regime exists, *J. Membrane Science* **256**, 57–63, 2005.

[20] K. Landman, M. McGuinness, Mean action time for diffusive processes, *Journal of Applied Mathematics and Decision Sciences* **4**(2), 125–141, 2000.

[21] X. Lu, P. Tervola, M. Viljanen, Transient analytical solution to heat conduction in a composite circular cylinder, *Int. J. Heat Mass Transfer* **49**, 341–348, 2006.

[22] F. Martelli, A. Sassaroli, S. Del Bianco, G. Zaccanti, Solution of the time-dependent diffusion equation for a three-layer medium: application to study photon migration through a simplified adult head model, *Phy. Med. Biol.* **52**, 2827–2843, 2007.

[23] MATLAB®, The MathWorks Inc., Natick, Massachusetts, `http://www.mathworks.com/products/matlab/`.

[24] M. McGuinness, W. L. Sweatman, D. Y. Baowan, S. I. Barry, Annealing

steel coils, *MISG 2008 Proceedings*, ed: T. Marchant, M. Edwards, G. N. Mercer, 2009.

[25] A. McNabb, G. C. Wake, Heat conduction and finite measures for transition times between steady states, *IMA Journal of Applied Mathematics* **47**(2), 192–206, 1991.

[26] A. McNabb, Mean action times, time lags and mean first passage times for some diffusion problems, *Mathl. Comput. Modelling* **18**(10), 123–129, 1993.

[27] J. R. Miller, P. M. Weaver, Temperature profiles in composite plates subject to time-dependent complex boundary conditions, *Composite Structures* **59**, 267–278, 2003.

[28] F. de Monte, An analytic approach to the unsteady heat conduction processes in one-dimensional composite media, *Int. J. Heat Mass Transfer* **45**, 1333–1343, 2002.

[29] F. de Monte, Transient heat conduction in one-dimension composite slab. A natural analytic approach, *Int. J. Heat Mass Transfer* **43**, 3607–3619, 2000.

[30] G. Oturanc, A. Z. Sahin, Eigenvalue analysis of temperature distribution in composite walls, *Int J. Energy Res.* **25**, 1189–1196, 2001.

[31] G. Pontrelli, F. de Monte, Mass diffusion through two-layer porous media: an application to the drug-eluting stent, *Int. J. Heat Mass Transfer* **50**, 3658–3669, 2007.

[32] Y. Sun, I. S. Wichman, On transient heat conduction in a one-dimensional composite slab, *Int. J Heat Mass Transfer* **47**, 1555–1559, 2004.

[33] W. Y. D. Yuen, Transient temperature distribution in a multilayer medium subject to radiative surface cooling, *Appl. Math. Modelling* **18**, 93–100, 1994.

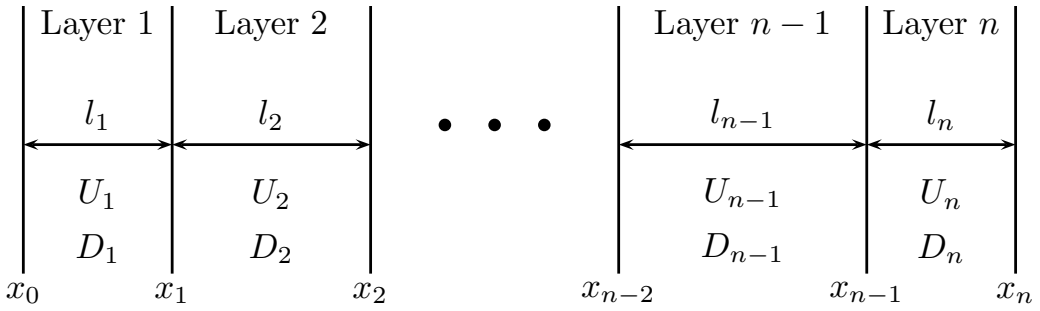

Figure 1: Multilayer schematic showing the nomenclature. Here U_i is the temperature in layer i at time t, D_i is the diffusivity of a given layer and l_i is the width of the layer.

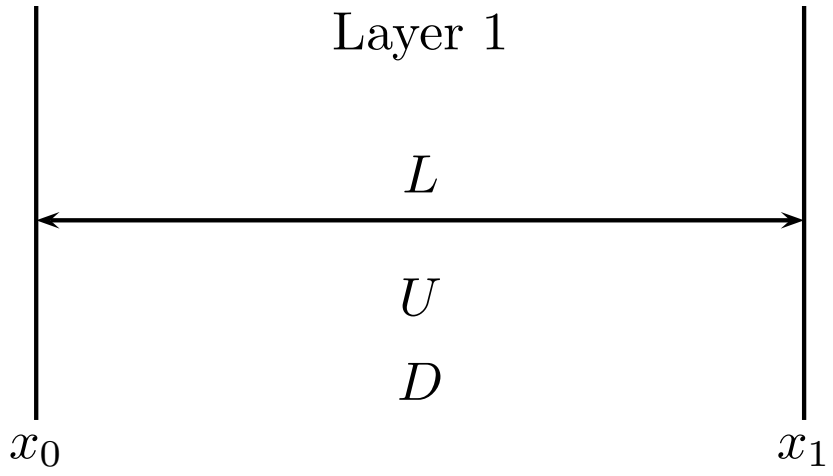

Figure 2: Single layer diffusion for $U(x,t)$, length L, and a single diffusivity, D.

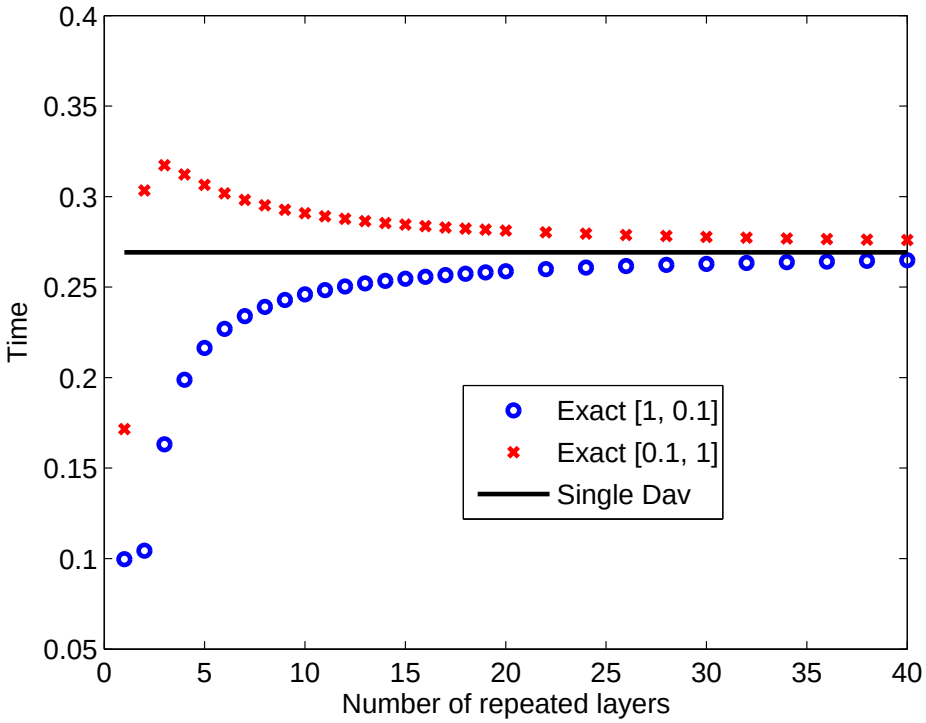

Figure 3: Critical time versus number of repeated layers for a multilayer medium. Results are calculated numerically using Equation (59). Here $L = 1$, $l_i = 1/n$, $\alpha = 0.5$, $a_1 = 1$, $b_1 = 0$, $\theta_1 = 1$, $a_2 = 1$, $b_2 = 0$, $\theta_2 = 0$ and $f_i = 0$. Diffusivities are either [1, 0.1] or [0.1, 1]. 'Single Dav' uses the single layer critical time, Equation (20), with $D_{\text{av}} = 0.18$ from Equation (4).

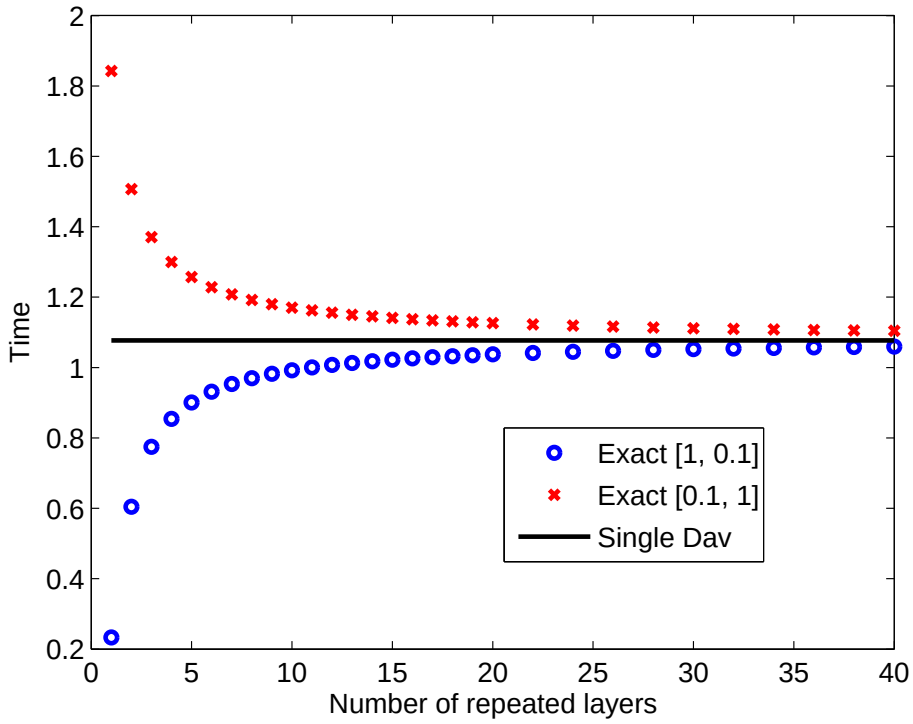

Figure 4: Critical time versus number of repeated layers for a multilayer medium. Results are calculated numerically using Equation (59). Here $L = 1$, $l_i = 1/n$, $\alpha = 0.5$, $a_1 = 1$, $b_1 = 0$, $\theta_1 = 1$, $a_2 = 0$, $b_2 = 1$, $\theta_2 = 0$ and $f_i = 0$. Diffusivities are either [1, 0.1] or [0.1, 1]. 'Single Dav' uses the second single layer critical time, Equation (21), with $D_{\text{av}} = 0.18$ from Equation (4).

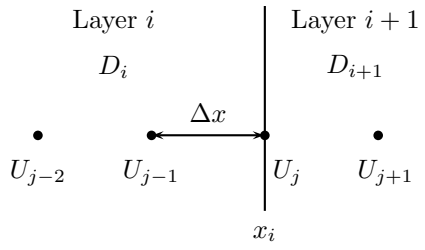

Figure 5: Finite difference scheme indexing where i denotes the layer and j denotes the spatial discretisation.